Functional analysis of novel polymorphisms in the human *SLCO1A2* gene that encodes the transporter OATP1A2

Fanfan Zhou[1], Jian Zheng[1,2], Ling Zhu[3], Andreas Jodal[1], Pei H. Cui[1,4], Mark Wong[5], Howard Gurney[5], W. Bret Church[1] and Michael Murray[1,4]

[1] *Faculty of Pharmacy, The University of Sydney, NSW 2006, Australia*

[2] *Alkali Soil Natural Environmental Science Center, Northeast Forestry University/Key Laboratory of Saline-alkali Vegetation Ecology Restoration in Oil Field, Ministry of Education, Harbin, 150040, China*

[3] *Retinal Therapeutics Research Group, Save Sight Institute, the University of Sydney, Sydney, NSW 2000, Australia*

[4] *Discipline of Pharmacology, School of Medical Sciences, The University of Sydney, NSW 2006, Australia*

[5] *Department of Medical Oncology, Westmead Hospital, Sydney, NSW 2145, Australia*

Running title: Functional characterization of novel OATP1A2 polymorphisms

Address for correspondence: Dr Fanfan Zhou,

Faculty of Pharmacy,

The University of Sydney,

Sydney, NSW, 2006, Australia

Email: fanfan.zhou@sydney.edu.au

Tel: 61-2-9036-3015

Fax: 61-2-9036-3244

Abbreviations: OATP1A2, organic anion transporting polypeptide 1A2; E3S, estrone-3-sulfate; GlpT, glycerol 3-phosphate transporter; PBS, phosphate-buffered saline; SLCO, solute carrier organic anion transporter; SNP, single nucleotide polymorphism.

ABSTRACT

Introduction: The solute carrier organic anion transporting polypeptide 1A2 (OATP1A2, *SLCO1A2*) is implicated in the cellular influx of a number of drugs.

Methods and Materials: We identified five novel single nucleotide polymorphisms (SNPs) in coding exons of the *SLCO1A2* gene in a cohort of subjects: G550A, G553A, G673A, A775C and G862A, that encoded the OATP1A2 variants E184K, D185N, V255I, T259P and D288N, respectively. The function and expression of these variant transporters were assessed in the HEK-293 cells.

Results and Discussion: We found that the novel variants, E184K, D185N, T259P and D288N, were associated with impaired estrone-3-sulfate, imatinib and methotrexate transport (~20%-50% of wild type control); function was retained by OATP1A2-V255I. From biotinylation assays the decreased function of these variants was due, at least in part, to impaired plasma membrane expression. The four loss-of-function variants were studied further using mutagenesis to produce variants that encode residues with different charges or steric properties. From immunoblotting, the replacement of negatively charged residues at amino acid positions 184 and 185 impaired membrane expression, while either a positive or negative charge at residue 288 supported the correct membrane targeting of OATP1A2. Replacement of T259 with bulky residues disrupted transporter stability. From molecular models E184, D185 and D288 were located near several charged residues such that intramolecular ionic interactions may stabilize the transporter structure.

Conclusion: Individuals who carry these novel SNPs in the *SLCO1A2* gene may be at risk from impaired efficacy or enhanced toxicity during treatment with drugs that are substrates for OATP1A2.

Keywords: Organic anion transporting polypeptide 1A2; *SLCO1A2*; polymorphisms; transporter variants.

Introduction

Organic anion transporting polypeptides (OATPs), encoded by the *SLCO* gene family, are expressed in epithelial cells from multiple tissues and mediate the cellular influx of organic anions, including a number of clinically important drugs. Because OATPs influence drug absorption, distribution and elimination, factors that impair function may influence therapeutic efficacy and toxicity (1-3). An important source of impaired function is pharmacogenetic variation caused by single nucleotide polymorphisms (SNPs) that alter the primary amino acid sequence of the encoded transporter. Thus, naturally occurring genetic variants in *SLCO* transporter genes may contribute to variable patient responses to certain drugs.

OATP1A2 (*SLCO1A2*) is an important member of the OATP transporter family that is expressed at the apical surface of the intestinal epithelium and renal tubules, in brain capillary endothelium and in biliary cholangiocytes (3-9). OATP1A2 participates in the intestinal absorption of drug substrates (3, 4), facilitates the tubular reabsorption of xenobiotics from urine as well as their secretion in bile (5) and may also influence uptake of drugs into brain (7). Endogenous substrates of OATP1A2 include bile acids, steroid and thyroid hormones, and their conjugates. Important drug substrates include imatinib, fexofenadine, methotrexate, HIV protease inhibitors, HMG-CoA reductase inhibitors, and certain peptides (3, 7, 10-14). Several studies have shown that the cellular uptake and pharmacokinetic behavior of some drugs may be impaired in the case of certain OATP1A2 variants (3, 9).

A number of studies have characterized the impact of pharmacogenetic variation in SLC transporters and their impact on transport function. Several naturally occurring SNPs in genes encoding OATPs have been identified that affect function (3, 15-21). Limited information is available on how polymorphisms alter the function of OATP1A2 (3, 9). Given the substrate specificity and expression of OATP1A2 in organs of importance to drug disposition and response, genetic variations in *SLCO1A2* may have significant pharmacologic and toxicological consequences. In the present study the coding exons in the *SLCO1A2* gene were sequenced in genomic DNA from a previously described cohort of subjects (22) and five novel variants were identified. The impact of the newly

id4entified SNPs on OATP1A2 transporter function and expression was assessed in cells. Particular amino acid residues in putative intracellular loops that are subject to pharmacogenetic variation were identified that have critical roles in the stability and membrane expression of the transporter. Together these findings identify new roles in intracellular amino acid residues that direct OATP1A2 to the plasma membrane.

Materials and Methods

Materials

[^{3}H] Estrone sulfate (E3S; specific activity 57.3 Ci/mmol) was purchased from PerkinElmer (Melbourne, VIC, Australia), [^{3}H] methotrexate (MTX; specific activity 15.7Ci/mmol) was purchased from BioScientific (Kirrawee, NSW, Australia) and [^{14}C]-imatinib (specific activity 51 mCi/mmol) was generously provided by Novartis (North Ryde, NSW, Australia). Culture media was obtained from Thermo Scientific (Lidcombe, NSW, Australia). Chloroquine, leupeptin, pepstatin and lactacystin were purchased from Sapphire Biosciences (Redfern, NSW, Australia). Unless otherwise stated all other chemicals and biochemicals were purchased from Sigma-Aldrich (Castle Hill, NSW, Australia).

Novel pharmacogenomics variants of SLCO1A2 and expressing in HEK-293 cells

The present study was approved by Institutional ethics committees of the Western Sydney Area Health Service and the University of Sydney, and conformed to the Declaration of Helsinki. (22). DNA was isolated from whole blood taken from 22 human subjects who had previously received imatinib (22). Resequencing of all coding exons in the SLCO1A2 gene was undertaken using KAPA HiFi PCR Kits (Geneworks, Hindmarsh SA, Australia). The primers used in amplification of the SLCO1A2 gene are shown in Table 1. Amplified DNA was purified on Wizard SV Gel and PCR clean up system (Promega, Alexandria, NSW, Australia) and subjected to bidirectional sequencing (Ramaciotti Centre for Gene Function Analysis, Randwick, NSW, Australia).

The *SLCO1A2* cDNA was purchased from GeneCopoeia (Cat. NO: GC-Q0577). Specific nucleotide changes were generated using Pfu DNA polymerase (Promega,

Alexandria, NSW, Australia) following the manufacturer's instructions. All sequences were confirmed by the dideoxy chain termination method (Ramaciotti Centre for Gene Function Analysis). HEK-293 cells were maintained at 37°C and 5% CO_2 in Dulbecco's modified Eagle's medium supplemented with 10% fetal calf serum. Cells were transfected with plasmid DNA using Lipofectamine 2000 Reagent (Invitrogen, Mount Waverley, VIC, Australia) following the manufacturer's instructions. Twenty-four h after transfection substrate uptake activities were measured.

Transport Studies

Cellular uptake of [^{3}H]-E3S (final concentration 0.3 μM, 67 nCi/well) in HEK-293 cells was conducted at 25^{o}C as described previously (11, 23). Uptake was initiated in phosphate-buffered saline (PBS; 137 mM NaCl, 2.7 mM KCl, 4.3 mM Na_2HPO_4, 1.4 mM KH_2PO_4, pH 7.4) containing 1 mM $CaCl_2$, and 1 mM $MgCl_2$, and was terminated by rapidly washing the cells in buffer at 4^{o}C. Preliminary experiments indicated that initial rates of OATP1A2-mediated substrate uptake in HEK293 cells were linear over at least 8 min, which was the time selected for subsequent experiments. The cells were then solubilized in 0.2 M NaOH, neutralized with 0.2 M HCl, and aliquoted for liquid scintillation counting. The uptake of [^{14}C]-imatinib (final concentration 3 μM, 6.1 nCi/well) was undertaken in analogous fashion at 37^{o}C in buffer contained 125 mM NaCl, 4.8 mM KCl, 5.6 mM D-glucose, 1.2 mM $CaCl_2$, 1.2 mM KH_2PO_4, 1.2 mM $MgSO_4$ and 25 mM HEPES (pH 5.0). The uptake of [^{3}H] MTX (final concentration 5 μM, 94 nCi/well) was performed in PBS (pH 5.5; 25^{o}C). Uptake was standardized to the amount of protein in each well. Kinetic studies were performed with varying concentrations of E3S (0.05-80 μM) added to the uptake buffer for a 4 min incubation in cells and apparent K_m and V_{max} values for transporter activity were then calculated where possible (GraphPad Prism 5.0; GraphPad Inc, LaJolla, CA, USA).

Cell-surface biotinylation

Cell-surface expression of OATP1A2 and variants was determined using the membrane impermeable biotinylation reagent NHS-SS-biotin (Quantum Scientific, Lane Cove West, NSW, Australia). Transporter cDNAs were expressed in HEK-293 cells in six-well plates

using Lipofectamine 2000, as previously described (24). After 24 h, the medium was removed and the cells were washed with ice-cold PBS (pH 8.0; 3 mL). Cells were incubated on ice with 1 mL of freshly prepared NHS-SS-biotin (0.5 mg in PBS) for 30 min with gentle shaking. After biotinylation, cells were washed with PBS containing 100 mM glycine (3 mL) and then incubated on ice for 20 min to ensure complete quenching of the unreacted NHS-SS-biotin. The cells were then treated for 30 min with lysis buffer (10 mM Tris, 150 mM NaCl, 1 mM EDTA, 0.1% SDS, 1% Triton X-100, that contained the protease inhibitors phenylmethylsulfonyl fluoride, 200 mg/mL, and leupeptin, 3 mg/mL, pH 7.4; 400 µL). Unlysed cells were removed by centrifugation at 14,000g at 4°C. Streptavidin-agarose beads (50 µL; Quantum Scientific) were then added to the supernatant to isolate biotinylated cell membrane proteins.

Electrophoresis and immunoblotting

Protein samples were denatured, loaded onto 7.5% polyacrylamide minigels and electrophoresed using a mini cell (Bio-Rad, Gladesville, NSW, Australia). Proteins were transferred to polyvinylidene fluoride membranes in an electroelution cell (Bio-Rad) and blocked for 1 h with 5% nonfat dry milk in PBS-Tween (80 mM Na_2HPO_4, 20 mM KH_2PO_4, 100 mM NaCl, and 0.05% Tween 20, pH 7.5), washed, and then incubated overnight at 4°C with anti-OATP1A2 antibody (1 µg/mL; ThermoFisher Scientific, Scoresby, VIC, Australia; Cat. No: sc-48744). The membranes were washed, incubated with goat anti-rabbit IgG conjugated to horseradish peroxidase (1:5000; Sapphire Biosciences, Cat. No: sc-2004), and signals were detected using the Immobilon Western Chemiluminescent HRP Substrate (Merck Millipore, Kilsyth, VIC, Australia).

Immunofluorescence of Transfected Cells

Cells in which OATP1A2 and its variants were over-expressed were washed three times in PBS, fixed for 20 min at room temperature in 4% paraformaldehyde in PBS, and then rewashed in PBS. The fixed cells were permeabilized with 0.1% Triton X-100 for 10 min, incubated for 30 min at room temperature in PBS containing 5% goat serum and then incubated for 2 h in the same medium containing anti-OATP1A2 antibody (10 µg/mL).

The cells were washed, and bound primary antibody was detected using Alexa Fluor® 594 conjugate goat anti-rabbit IgG (Invitrogen Cat. No: A11012; 1:1000 dilution; 1 h). Treated cells were washed thoroughly, and the cover glasses were mounted in VECTASHIELD Mounting Medium (Abacus ALS, East Brisbane QLD, Australia). Samples were visualized with a Leica DMI3000 B epi fluorescence microscope (Leica Microsystems, North Ryde, NSW, Australia).

Computer modeling

3D structures of bacterial transporters were used in the present study as templates for modeling OATP1A2. In the most straightforward arrangement of the transporter structures, the 12 helices were arranged as a pair of distinct 6 helix bundles using the glycerol-3-phosphate transporter from *E coli* as template (GlpT, 1PW4) (25).

Multiple sequence alignments were performed using CLUSTAL (26) as implemented in the European Bioinformatics Institute resource (27). The sequence alignment retaining the transmembrane boundary predictions and template were used as inputs for the comparative protein modeling software MODELLER (28), using the graphical interface of Discovery Studio (v3.0, Accelrys, San Diego, CA, USA). The extended fifth extracellular loop between helices 9 and 10 (~105 amino acids) in the structure of OATP1A2 was least reliably modeled and was removed to prior to the analysis, along with the N- and C-termini that also do not align with the GlpT template.

Statistics

Data are presented throughout as mean±SEM. The Student's *t*-test was used to test for differences between two sets of normally distributed data. Differences in transport function of OATP1A2 and multiple variants were detected by one-way analysis of variance and Dunnett's Testing.

Results

Identification of *SLCO1A2* polymorphisms in a patient cohort

Genomic DNA from twenty-two subjects was subjected to bidirectional resequencing of all coding exons of the *SLCO1A2* gene (exons 3-16) using the primers detailed in Table 1; exons 1 and 2 in *SLCO1A2* are non-coding exons. In total, five nonsynonymous SNPs were identified in the patient cohort (allele frequencies and demographic factors are shown in Table 2). Two of the five novel SNPs in the *SLCO1A2* gene (G763A and G862A in exon 9), that encoded the OATP1A2-V255I and OATP1A2-D288N variant transporters, respectively, were found in three heterozygous individuals. One individual was homozygous for the SNP A775C in exon 9 that encoded OATP1A2-T259P. The two remaining SNPs in *SLCO1A2* were more widely distributed throughout the cohort. Thus, fourteen subjects were heterozygous for the G550A SNP in exon 7 that encoded OATP1A2-E184K (allele frequency 0.325) and nineteen were heterozygous for the G553A SNP in exon 7 (allele frequency 0.45) that encoded OATP1A2-D185N.

Functional analysis of novel *SLCO1A2* variants

In human embryonic kidney (HEK-293) cells, the transient transfection of cDNA encoding wild-type OATP1A2 increased the influx of the reference substrate [^{3}H]-E3S to ~11-fold of control (Fig. 1A), while the influx of [^{3}H]-MTX and [^{14}C]-imatinib was increased to ~3.3-fold and ~2.0-fold of respective control (Fig. 1B, 1C). Under the test conditions basal rates of substrate uptake by wild-type OATP1A2 were 12.5 pmol/(mg*min) for E3S, 57.5 pmol/(mg*min) for MTX and 53.8 pmol/(mg*min) for imatinib.

In order to assess the impact of the novel *SLCO1A2* variants on transporter function, HEK-293 cells were transfected with variant cDNAs that had been engineered by site-directed mutagenesis. Transport of the model substrate E3S by the variants OATP1A2-E184K, D185N, D288N and T259P was markedly altered compared to wild-type OATP1A2 (Fig. 1A). In the case of the OATP1A2-V255I variant transport function was slightly, but not significantly, decreased when E3S was the substrate. Compared to wild-type, influx of the OATP1A2 substrate imatinib by the five novel OATP1A2 variants was

also impaired (Fig. 1B). With the OATP1A2-E184K, -D185N, –T259P and –D288N variants the decrease in function was to ~40-50% of wild type control, while transport by OATP1A2-V255I was only slightly decreased (Fig. 1B). Similar trends were noted in MTX transport, with pronounced decreases observed for the variants, again with the exception of OATP1A2-V255I (Fig. 1C).

Altered cellular expression of the novel variants of OATP1A2

The mechanism underlying the decrease in the transport function of the novel OATP1A2 variants was assessed initially in transporter biotinylation and immunoblotting analyses in transfected HEK-293 cells. From densitometric analysis, the plasma membrane expression of the E184K, D185N, T259P and D288N variants was decreased markedly to ~20%-40% of wild type, whereas the expression of the V255I variant was unchanged (Fig. 1D). In confirmatory immunocolocalization experiments the expression of OATP1A2-E184K, D185N, T259N and D288N variants at the plasma membrane was decreased (Fig. 2). The specificity of biotinylation was confirmed by reprobing the immunoblotting membranes with an anti-actin antibody.

Apart from impaired expression at the cell surface, transport function could also be decreased due to altered substrate affinity or turnover. Kinetic analysis of E3S transport was conducted in HEK-293 cells that expressed wild-type OATP1A2 and the D288N-variant. Compared with wild-type the variant exhibited decreased apparent K_m (12±1 compared with 20±3 μM) and V_{max} values (16.7±0.4 versus 36.7±1.8 pmol/μg protein*4 min), which led to an approximate 25% decline in intrinsic clearance (V_{max}/K_m). Because the other novel OATP1A2 variants (E184K, D185N and T259P) had low transporter function conventional kinetic studies could not be conducted.

Functional analysis of further mutants derived from the novel OATP1A2 variants

Three of the four residues that were subject to naturally occurring polymorphisms in patient samples encoded acidic residues (E184, D185 and D288), while the fourth encoded the polar amino acid threonine (T259). Because the variant transporters all exhibited a loss-of-function we tested the hypothesis that these highly polar amino acids play important roles in OATP1A2 activity. We systematically mutagenized the residues

to evaluate the impact on transport function of amino acid replacement. As shown in Figures 3A and 3B, function was retained providing acidic residues (aspartic or glutamic acids) were located at 184 and 185, because basic residues (lysine, arginine or histidine), or the neutral polar asparagine, encoded variants with greatly decreased activity (7%-63% of wild-type control). Interestingly, and in contrast with the findings with residues 184/185, either acidic or basic residues (glutamic acid, lysine, arginine or histidine) at position 288 supported full transporter function (Fig 3D), while neutral polar (asparagine or glutamine) or hydrophobic (valine) residues impaired E3S transport.

The variant T259P, in which the neutral polar threonine residue is replaced by a rigid proline, also exhibited decreased function (to ~20% of wild-type control). We further mutagenized the threonine to histidine (basic), or tyrosine, phenylalanine and tryptophan (neutral aromatic) residues that all have bulky side chains, or to alanine that has a small side chain. Transporter function was only impaired with variant amino acids that contained bulky side chains (3%-43% of wild-type control) because the transport capacity of OATP1A2-T259A was similar to wild-type (Fig 3C). In summary, these observations indicate that an acidic amino acid is essential at positions 184 and 185, while either acidic or basic residues at position 288 allows function to be retained. Inclusion of bulky amino acids in place of the polar threonine at position 259 markedly decreases function.

To pursue potential mechanisms for the observed functional changes induced by replacement of the naturally occurring residues at these positions we investigated the expression of mutant transporters in whole cell lysates. From direct immunoblotting, signals corresponding to immunoreactive OATP1A2 protein were detected at ~65kD and ~90kD in lysates. Interestingly, because the total cell expression signal at ~90kD was decreased, particularly in the loss-of-function mutants engineered at residues 184, 185 and 259 (Fig. 4A-C), but not those at residue 288 (Fig 4D), it appeared likely that the first three of these residues may play critical roles in maintaining the stability of the OATP1A2 protein.

Computational modeling of OATP1A2

A crystal structure for OATP1A2 is not currently available but 3D structures of bacterial transporters have been reported and exhibit the basic topology proposed for human transporters (24, 25, 29, 30).

To provide the most straightforward analysis, the 12 transmembrane domain helices in the arrangement, in which there were two separately identifiable 6 helix bundles, was considered suitable. The glycerol 3-phosphate transporter (GlpT) from E. coli (PDB ID 1pw4) (25), which shares 8% sequence relatedness across the aligned regions, was selected as a suitable template (at 3.3 Å resolution). Model quality parameters determined by Molprobity were: rotamer outliers 7.1%, Ramachandran outliers 2.9%, Ramachandran favoured 91%, 34 Cβ deviations >0.25Å, residues with bad bonds 0.0%, and residues with bad angles 2.7% (31); this level of quality is suitable for the present purposes. As shown in Fig 5A, the residues E184 and D185 are within the second intracellular loop, while D288 is in the third intracellular loop and V255/T259 are in transmembrane helix six. Figs 5B and 5C show the putative conformation of OATP1A2 and provide spatial context for the E184, D185 and D288 residues.

Discussion

OATP1A2 is a major transporter responsible for the cellular influx of important drugs such as imatinib, MTX, fexofenadine and HMG-CoA reductase inhibitors (3, 7, 10, 12, 32-34). Pharmacogenetic variants of this transporter that have altered function may influence both the rate of drug influx and the toxicity of various agents in cells and *in vivo* (3, 9). The functional characterization and molecular evaluation of novel *SLCO1A2* genetic variants identified in patients could be significant for understanding inter-individual variation in the response to drug substrates.

The functional significance of five novel *SLCO1A2* variants that were identified in a cohort of subjects was evaluated *in vitro*. Following transient transfection of the variant cDNAs into HEK-293 cells, transporter function and plasma membrane expression were determined. Variants that had decreased substrate transport activity also exhibited a corresponding decline in expression at the plasma membrane.

One of the novel variants identified in the present study (*SLCO1A2* G862A) encodes the variant residue D288N that is located within the large putative third intracellular loop between transmembrane domains 6 and 7. Three other *SLCO1A2* variants that led to sequence changes in this loop have been identified previously (3). The truncated variant transporter OATP1A2-N278X was inactive, but neither OATP1A2-T277N nor I281V exhibited altered function with E3S or MTX (3). The present studies suggested that transporter function and membrane expression were decreased in the case of the D288N variant so that it is likely that this residue is important in membrane targeting. It is feasible that this residue may interact with an intracellular chaperone protein that directs OATP1A2 to the plasma membrane or that intramolecular interactions between residues stabilize the conformation of the transporter; the present investigation focused principally on the second possibility. From modeling considerations the location of D288 may facilitate interactions with nearby basic residues in the large intracellular loop (such as K283, K289 or K291) or adjacent loops (such as K188 in intracellular loop 2 or K544 in intracellular loop 5). It also emerged that replacement of D288 with basic amino acids retained E3S transport capacity and high plasma membrane expression. Again, a number of negatively charged residues, such as E285, E287, E292 and E293 are also

in the vicinity of D288 and several others are present in adjacent loops. However, it is important to add that the large intracellular loop, and the large extracellular loop between transmembrane domains 9 and 10, are least reliably predicted by modeling and conformations other than that shown in Fig 5 are possible.

Apart from OATP1A2-D288N, two other variants - OATP1A2-E184K and OATP1A2-D185N - exhibited decreased cellular uptake of E3S, MTX and imatinib. The functional impairment in the cases of these two variants might be due to decreased cell surface and total cellular expression. From computer modeling, E184 and D185 were located within the second intracellular loop and could interact with adjacent positively charged residues, such as R85 in the first intracellular loop or K188, K295 and K296 in the second and third intracellular loops. Unlike the situation with D288, replacement of E184 and D185 with basic amino acids led to loss of function. Presumably this could be due to a shortage of nearby negatively charged residues that might stabilize the conformation, or alternately that the region near 184/185 may have a pivotal role in the transport mechanism. Thus, it is feasible that the native OATP1A2 protein might be stabilized by specific ionic interactions and that replacement of important residues disrupts the interactions and destabilizes the protein.

It has been suggested that transmembrane domain helices control membrane targeting, protein stability and substrate binding in SLC transporters (24, 35-37). In the case of residue T259, which is located in transmembrane domain 6, the present data suggest that the steric nature of the amino acid at this position is an important factor. While the residues threonine (polar amino acid) and alanine (small, hydrophobic amino acid) sustained transporter function and stability, the larger or more rigid histidine, tyrosine, phenylalanine, proline and tryptophan strongly disrupted transport function, perhaps by altering the conformation of the protein.

Previous studies of the impact of pharmacogenetic variants of OATP1A2 on drug transport have yielded variable findings. Thus, imatinib uptake was decreased in cells containing the OATP1A2 variants *3 (E172D in transmembrane domain 4), *5 and *6 (N128Y and N135I in intracellular loop 2), but not the *7 variant (T668S in the C-terminal region) (23). Uptake of E3S and two peptide substrates was markedly impaired

in the case of the *3 and *6 variants but less so with *5 and *7 (9). This resembled the present findings in relation to negatively charged intracellular residues in OATP1A2. Interestingly, similar findings have been noted with acidic intracellular residues in other SLC transporters. Thus, mutagenesis of acidic residues in the large intracellular loop in the human dipeptide transporter (hPEPT1; *SLC15A1*) and the E452K substitution in the C-terminus of the organic cation/carnitine transporter-2 (OCTN2; *SLC22A5*) also produced marked decreases in substrate transport (38, 39). It would now be of interest to evaluate in greater detail the incidence of pharmacogenetic variation in acidic residues in intracellular loops in human SLC transporters.

Conclusion

The tissue expression pattern of OATP1A2 is significant for tissue-specific drug disposition. Location in the distal tubules of nephrons, intestinal villi and endothelial cells that constitute the blood-brain barrier is clinically relevant, especially in view of the broad substrate specificity for this transporter. The present identification of novel variants of OATP1A2 that have impaired function and expression could affect the disposition of endogenous compounds and drugs in multiple tissues and contribute to inter-individual variability in drug responsiveness and toxicity. In this regard it is noteworthy that the very recent study by Angelini et al., reported that there were significant relationships between major and complete molecular responses in 189 imatinib-treated patients with chronic myelogenous leukemia and the presence of pharmacogenetic variation in several SLC transporters, including OATP1A2 (40).

Acknowledgements

Special thanks to Avy Sim for assistance with the computer modeling of OATP1A2 structure. This study was supported by grants from Cancer Council NSW and the Australian National Health and Medical Research Council. The generous gifts of imatinib and ^{14}C-imatinib from Novartis are gratefully acknowledged.

Disclosure of Potential Conflicts of Interest

The authors declare no conflict of interest.

Reference

1. Poirier A, Funk C, Lave T, Noe J. New strategies to address drug-drug interactions involving OATPs. Curr Opin Drug Discov Devel. 2007 Jan;10(1):74-83.

2. Kivisto KT, Niemi M. Influence of drug transporter polymorphisms on pravastatin pharmacokinetics in humans. Pharm Res. 2007 Feb;24(2):239-47.

3. Badagnani I, Castro RA, Taylor TR, Brett CM, Huang CC, Stryke D, et al. Interaction of methotrexate with organic-anion transporting polypeptide 1A2 and its genetic variants. J Pharmacol Exp Ther. 2006 Aug;318(2):521-9.

4. Glaeser H, Bailey DG, Dresser GK, Gregor JC, Schwarz UI, McGrath JS, et al. Intestinal drug transporter expression and the impact of grapefruit juice in humans. Clin Pharmacol Ther. 2007 Mar;81(3):362-70.

5. Roth M, Obaidat A, Hagenbuch B. OATPs, OATs and OCTs: the organic anion and cation transporters of the SLCO and SLC22A gene superfamilies. Br J Pharmacol. 2012 Mar;165(5):1260-87.

6. Yang CH, Glover KP, Han X. Characterization of cellular uptake of perfluorooctanoate via organic anion-transporting polypeptide 1A2, organic anion transporter 4, and urate transporter 1 for their potential roles in mediating human renal reabsorption of perfluorocarboxylates. Toxicol Sci. 2010 Oct;117(2):294-302.

7. Gao B, Hagenbuch B, Kullak-Ublick GA, Benke D, Aguzzi A, Meier PJ. Organic anion-transporting polypeptides mediate transport of opioid peptides across blood-brain barrier. J Pharmacol Exp Ther. 2000 Jul;294(1):73-9.

8. Su Y, Zhang X, Sinko PJ. Human organic anion-transporting polypeptide OATP-A (SLC21A3) acts in concert with P-glycoprotein and multidrug resistance protein 2 in the vectorial transport of Saquinavir in Hep G2 cells. Mol Pharm. 2004 Jan 12;1(1):49-56.

9. Lee W, Glaeser H, Smith LH, Roberts RL, Moeckel GW, Gervasini G, et al. Polymorphisms in human organic anion-transporting polypeptide 1A2 (OATP1A2): implications for altered drug disposition and central nervous system drug entry. J Biol Chem. 2005 Mar 11;280(10):9610-7.

10. Hartkoorn RC, Kwan WS, Shallcross V, Chaikan A, Liptrott N, Egan D, et al. HIV protease inhibitors are substrates for OATP1A2, OATP1B1 and OATP1B3 and lopinavir plasma concentrations are influenced by SLCO1B1 polymorphisms. Pharmacogenet Genomics. 2010 Feb;20(2):112-20.

11. Hu S, Franke RM, Filipski KK, Hu C, Orwick SJ, de Bruijn EA, et al. Interaction of imatinib with human organic ion carriers. Clin Cancer Res. 2008 May 15;14(10):3141-8.

12. Kullak-Ublick GA, Hagenbuch B, Stieger B, Schteingart CD, Hofmann AF, Wolkoff AW, et al. Molecular and functional characterization of an organic anion transporting polypeptide cloned from human liver. Gastroenterology. 1995 Oct;109(4):1274-82.

13. Mandery K, Bujok K, Schmidt I, Keiser M, Siegmund W, Balk B, et al. Influence of the flavonoids apigenin, kaempferol, and quercetin on the function of organic anion transporting polypeptides 1A2 and 2B1. Biochem Pharmacol. 2010 Dec 1;80(11):1746-53.

14. Shirasaka Y, Suzuki K, Nakanishi T, Tamai I. Intestinal absorption of HMG-CoA reductase inhibitor pravastatin mediated by organic anion transporting polypeptide. Pharm Res. 2010 Oct;27(10):2141-9.

15. Nies AT, Niemi M, Burk O, Winter S, Zanger UM, Stieger B, et al. Genetics is a major determinant of expression of the human hepatic uptake transporter OATP1B1, but not of OATP1B3 and OATP2B1. Genome Med. 2013 Jan 11;5(1):1.

16. Rodrigues AC, Perin PM, Purim SG, Silbiger VN, Genvigir FD, Willrich MA, et al. Pharmacogenetics of OATP Transporters Reveals That SLCO1B1 c.388A>G Variant Is Determinant of Increased Atorvastatin Response. Int J Mol Sci. 2011;12(9):5815-27.

17. Thakkar N, Kim K, Jang ER, Han S, Kim D, Merchant N, et al. A cancer-specific variant of the SLCO1B3 gene encodes a novel human organic anion transporting polypeptide 1B3 (OATP1B3) localized mainly in the cytoplasm of colon and pancreatic cancer cells. Mol Pharm. 2013 Jan 7;10(1):406-16.

18. Picard N, Yee SW, Woillard JB, Lebranchu Y, Le Meur Y, Giacomini KM, et al. The role of organic anion-transporting polypeptides and their common genetic variants in mycophenolic acid pharmacokinetics. Clin Pharmacol Ther. 2010 Jan;87(1):100-8.

19. Tsuda-Tsukimoto M, Maeda T, Iwanaga T, Kume T, Tamai I. Characterization of hepatobiliary transport systems of a novel alpha4beta1/alpha4beta7 dual antagonist, TR-14035. Pharm Res. 2006 Nov;23(11):2646-56.

20. Ho RH, Tirona RG, Leake BF, Glaeser H, Lee W, Lemke CJ, et al. Drug and bile acid transporters in rosuvastatin hepatic uptake: function, expression, and pharmacogenetics. Gastroenterology. 2006 May;130(6):1793-806.

21. Kameyama Y, Yamashita K, Kobayashi K, Hosokawa M, Chiba K. Functional characterization of SLCO1B1 (OATP-C) variants, SLCO1B1*5, SLCO1B1*15 and SLCO1B1*15+C1007G, by using transient expression systems of HeLa and HEK293 cells. Pharmacogenet Genomics. 2005 Jul;15(7):513-22.

22. Gurney H, Wong M, Balleine RL, Rivory LP, McLachlan AJ, Hoskins JM, et al. Imatinib disposition and ABCB1 (MDR1, P-glycoprotein) genotype. Clin Pharmacol Ther. 2007 Jul;82(1):33-40.

23. Eechoute K, Franke RM, Loos WJ, Scherkenbach LA, Boere I, Verweij J, et al. Environmental and genetic factors affecting transport of imatinib by OATP1A2. Clin Pharmacol Ther. 2011 Jun;89(6):816-20.

24. Zhou F, Zhu L, Cui PH, Church WB, Murray M. Functional characterization of nonsynonymous single nucleotide polymorphisms in the human organic anion transporter 4 (hOAT4). Br J Pharmacol. 2010 Jan 1;159(2):419-27.

25. Huang Y, Lemieux MJ, Song J, Auer M, Wang DN. Structure and mechanism of the glycerol-3-phosphate transporter from Escherichia coli. Science. 2003 Aug 1;301(5633):616-20.

26. Thompson JD, Higgins DG, Gibson TJ. CLUSTAL W: improving the sensitivity of progressive multiple sequence alignment through sequence weighting, position-specific gap penalties and weight matrix choice. Nucleic Acids Res. 1994 Nov 11;22(22):4673-80.

27. Labarga A, Valentin F, Anderson M, Lopez R. Web services at the European bioinformatics institute. Nucleic Acids Res. 2007 Jul;35(Web Server issue):W6-11.

28. Sali A, Potterton L, Yuan F, van Vlijmen H, Karplus M. Evaluation of comparative protein modeling by MODELLER. Proteins. 1995 Nov;23(3):318-26.

29. Perry JL, Dembla-Rajpal N, Hall LA, Pritchard JB. A three-dimensional model of human organic anion transporter 1: aromatic amino acids required for substrate transport. J Biol Chem. 2006 Dec 8;281(49):38071-9.

30. Meier-Abt F, Mokrab Y, Mizuguchi K. Organic anion transporting polypeptides of the OATP/SLCO superfamily: identification of new members in nonmammalian species, comparative modeling and a potential transport mode. J Membr Biol. 2005 Dec;208(3):213-27.

31. Davis IW, Leaver-Fay A, Chen VB, Block JN, Kapral GJ, Wang X, et al. MolProbity: all-atom contacts and structure validation for proteins and nucleic acids. Nucleic Acids Res. 2007 Jul;35(Web Server issue):W375-83.

32. Eckhardt U, Schroeder A, Stieger B, Hochli M, Landmann L, Tynes R, et al. Polyspecific substrate uptake by the hepatic organic anion transporter Oatp1 in stably transfected CHO cells. Am J Physiol. 1999 Apr;276(4 Pt 1):G1037-42.

33. Jacquemin E, Hagenbuch B, Stieger B, Wolkoff AW, Meier PJ. Expression cloning of a rat liver Na(+)-independent organic anion transporter. Proc Natl Acad Sci U S A. 1994 Jan 4;91(1):133-7.

34. Kim RB, Leake B, Cvetkovic M, Roden MM, Nadeau J, Walubo A, et al. Modulation by drugs of human hepatic sodium-dependent bile acid transporter (sodium taurocholate cotransporting polypeptide) activity. J Pharmacol Exp Ther. 1999 Dec;291(3):1204-9.

35. Li N, Hong W, Huang H, Lu H, Lin G, Hong M. Identification of amino acids essential for estrone-3-sulfate transport within transmembrane domain 2 of organic anion transporting polypeptide 1B1. PLoS One. 2012;7(5):e36647.

36. Gui C, Hagenbuch B. Amino acid residues in transmembrane domain 10 of organic anion transporting polypeptide 1B3 are critical for cholecystokinin octapeptide transport. Biochemistry. 2008 Sep 2;47(35):9090-7.

37. Hong M, Li S, Zhou F, Thomas PE, You G. Putative transmembrane domain 12 of the human organic anion transporter hOAT1 determines transporter stability and maturation efficiency. J Pharmacol Exp Ther. 2010 Feb;332(2):650-8.

38. Xu L, Li Y, Haworth IS, Davies DL. Functional role of the intracellular loop linking transmembrane domains 6 and 7 of the human dipeptide transporter hPEPT1. J Membr Biol. 2010 Dec;238(1-3):43-9.

39. Amat di San Filippo C, Pasquali M, Longo N. Pharmacological rescue of carnitine transport in primary carnitine deficiency. Hum Mutat. 2006 Jun;27(6):513-23.

40. Angelini S, Soverini S, Ravegnini G, Barnett M, Turrini E, Thornquist M, et al. Association between imatinib transporters and metabolizing enzymes genotype and response in newly diagnosed chronic myeloid leukemia patients receiving imatinib therapy. Haematologica. 2013 Feb;98(2):193-200.

Table 1: Primers used in the sequencing of *SLCO1A2* gene exons

OATP1A2	**Forward primer (5'-3')**	**Reverse primer (5'-3')**
Exon 3	GCGTTCCAGGTATTTTTG	GTTAGAAACCCTGCAAG
Exon 4	CAATATTGAGGCTGCAACTG	GATGGAACCCTTAGTATCC
Exon 5	CCCTCTGTAAATGTTGGTG	GACCTTTTTGTCAATGTAAGC
Exon 6	GGTAGATCATCCACAGGCAG	CCTGGAGAGAGAACATATC
Exon 7	CACTTACACTTGTCCATAC	TGTAGTGCCAAGCAGATG
Exon 8	GTGACCCAGCATGAAAG	TAGAATTATCGGGTCCC
Exon 9	GATAGACAGATAACCAGCC	ACCATAGGAAGAATCGG
Exon 10	CCCAGTCAGCTACATCAC	GGTATTTCTGACCTCTTCC
Exon 11	GTGGGTAATGTGTAACTAAG	CAAAGACAATCATGCACAC
Exon 12	CTAACTGGGGATTGAGATGA	CACTGGTCAGATGCTATGG
Exon 13	GTTATATGGTGTAATCTTGAGAGAC	GGAAGAAAAGTAGCGAGGAATAG
Exon 14	CCCTGAATAACCAATAAGTGAGC	GACATTTGCTAGACTGCTTTTCTG
Exon 15	GTTGCATTTGACCATAAGATTAC	GAGAAGGCATTAGGAGAC
Exon 16	GGATTTTCTCAGTGGGA	AGCTGGCTCTAAGAATCT

Table 2. Demographic factors in the subject cohort and novel nonsynonymous SNPs of *SLCO1A2* identified in genomic DNA.

Gender: 12M, 10F

Age range: 38.3 – 68.8 yr

Ethnic ancestry: Caucasian 16, Asian 3, Pacific Islander 2, Hispanic 1

OATP1A2 Variant	Exon	Nucleic Acid Position	Allele Change	Allele Frequency
E184K	7	550	g=>a	0.325
D185N	7	553	g=>a	0.450
V255I	9	763	g=>a	0.075
T259P	9	775	a=>c	0.050
D288N	9	862	g=>a	0.075

Figure Legends

Fig 1. Transporter function and protein expression of OATP1A2 and its variants. A, B and C: Transport of 300 nM [^{3}H] estrone sulphate (E3S), 3 μM [^{14}C] imatinib and 5 μM [^{3}H] methotrexate (MTX) in HEK-293 cells transfected with wild type and mutagenized variants of OATP1A2, relative to mock-transfected control (MOCK). Basal rates of substrate uptake by wild-type OATP1A2 were 12.5 pmol/(mg*min) for E3S, 57.5 pmol/(mg*min) for MTX and 53.8 pmol/(mg*min) for imatinib. D: Western blot analysis of cell surface expression of wild-type OATP1A2 and its variant transporters. Upper panel: Cells were biotinylated, and the labeled cell surface proteins were precipitated with streptavidin beads and separated by gel electrophoresis, followed by Western blotting with anti-OATP1A2 antibody. Bottom panel: Densitometric analysis of transporter plasma expression. NC: negative control. Values are mean ± SE (n=3). Different from wild-type, * $p<0.05$; ** $p<0.01$.

Fig 2. Immunofluorescence analysis of OATP1A2 and its variants expressed in HEK-293 cells. Cells that over-expressed OATP1A2 and its variants were stained with anti-OATP1A2 antibody and Alexa Fluor® 594 conjugate goat anti-rabbit IgG. Panels A ,C, E, G, I and K show the specific immunostaining of OATP1A2, which appears as bright fluorescence. Panels B, D, F, H, J, and L are phase-contrast images and show that cells remain fully attached to the culture dishes under the test conditions. WT: wild-type.

Fig 3. Transporter function of the derivative mutants of OATP1A2. The transport of 300 nM [^{3}H] estrone sulphate (E3S) in HEK-293 cells transfected with wild type and derivative mutants of OATP1A2-E184 (A), -D185 (B), -T259 (C) and –D288 (D) (after subtraction of uptake in with mock-transfected control cells). Values are mean ± SE (n=3). Different from wild-type, * $p<0.05$; ** $p<0.01$;

Fig 4. Protein expression of OATP1A2 and its mutants in HEK-293 cells. Western blot analysis of wild-type OATP1A2 and derivative mutants created at amino acid position 184 (A), 185 (B), 259 (C) and 288 (D). Upper panels: Cell surface expression of OATP1A2 and its mutants. Cells were biotinylated, and the labeled cell surface proteins were precipitated with streptavidin beads and separated by gel electrophoresis, followed

by Western blotting with anti-OATP1A2 antibody. Middle panels: Western analysis of total cellular expression of OATP1A2 and its mutants. Lower panels: after stripping, blots were reprobed with anti-actin antibody. WT: wild-type, NC: negative control.

Fig 5. Computer modeling of OATP1A2 structure. (A) The topological structure of OATP1A2 obtained by Transmembrane Helix Benchmarking software (www.sydney.edu.au/pharmacy/sbio/software/TMH_benchmark) based on the structure of GlpT and shown in the same orientation. Circled residues indicate the location of the amino acid replacements in the five novel variants found in the current study. The N- and C-termini are located intracellularly while a series of extracellular and intracellular loops connect the trans-membrane domains, (B) Proposed overall 3D structure showing transmembrane (TM) helices, extracellular (EC) and intracellular (IC) loops, and (C) a close up view, in the same orientation, of the intracellular region near the large loop showing the charged side chains. T259 is shown (orange) in TM6 of the helix bundle. Charged amino acids of the intracellular regions are colored blue and red for basic and acidic residues, respectively. The figures were drawn using PyMOL (DeLano Scientific; San Carlos, CA, USA).

Figure 1

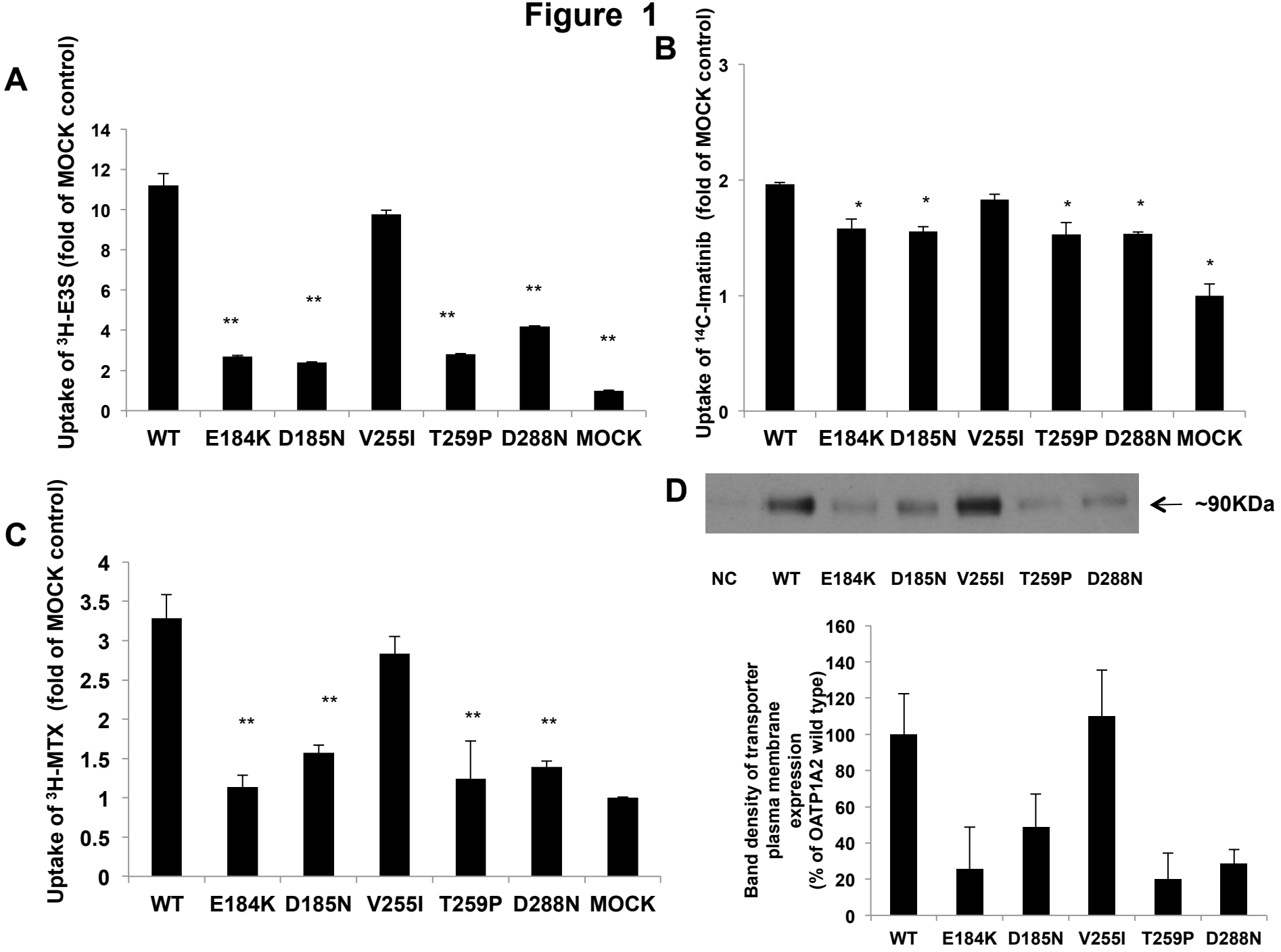
A
Uptake of ^{3}H-E3S (fold of MOCK control)
14
12
10
8
6
4
2
0
**
**
**
**
**
WT
E184K
D185N
V255I
T259P
D288N
MOCK
B
Uptake of ^{14}C-Imatinib (fold of MOCK control)
3
2
1
0
*
*
*
*
*
WT
E184K
D185N
V255I
T259P
D288N
MOCK
C
Uptake of ^{3}H-MTX (fold of MOCK control)
4
3.5
3
2.5
2
1.5
1
0.5
0
**
**
**
**
WT
E184K
D185N
V255I
T259P
D288N
MOCK
D
~90KDa
NC
WT
E184K
D185N
V255I
T259P
D288N
Band density of transporter plasma membrane expression (% of OATP1A2 wild type)
160
140
120
100
80
60
40
20
0
WT
E184K
D185N
V255I
T259P
D288N

Figure 2

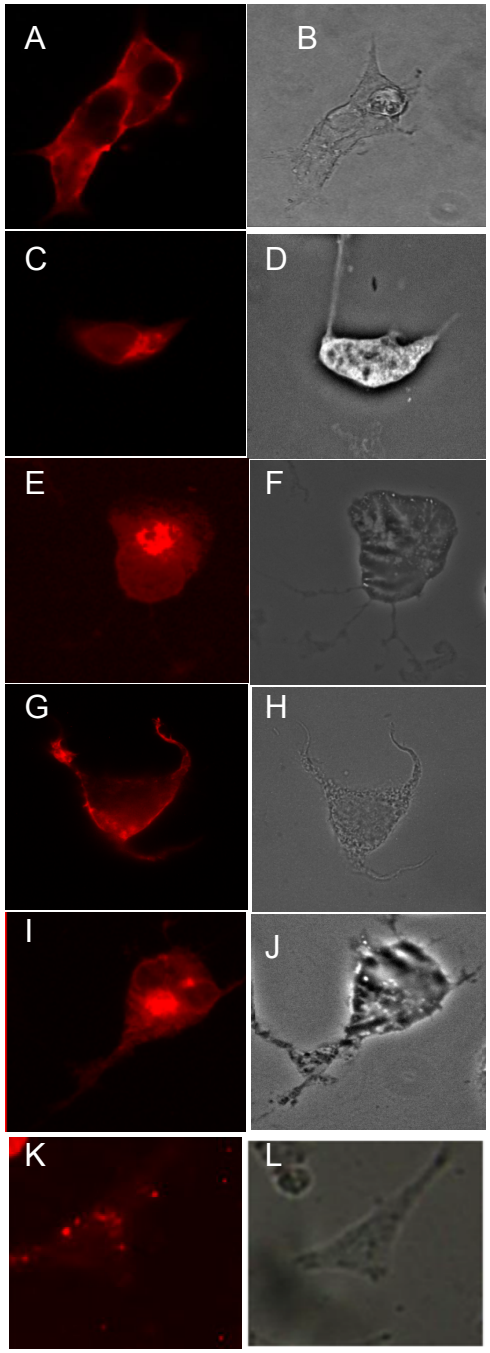

OATP1A2 WT

OATP1A2 E184K

OATP1A2 D185N

OATP1A2 T255I

OATP1A2 T259P

OATP1A2 D288N

Figure 3

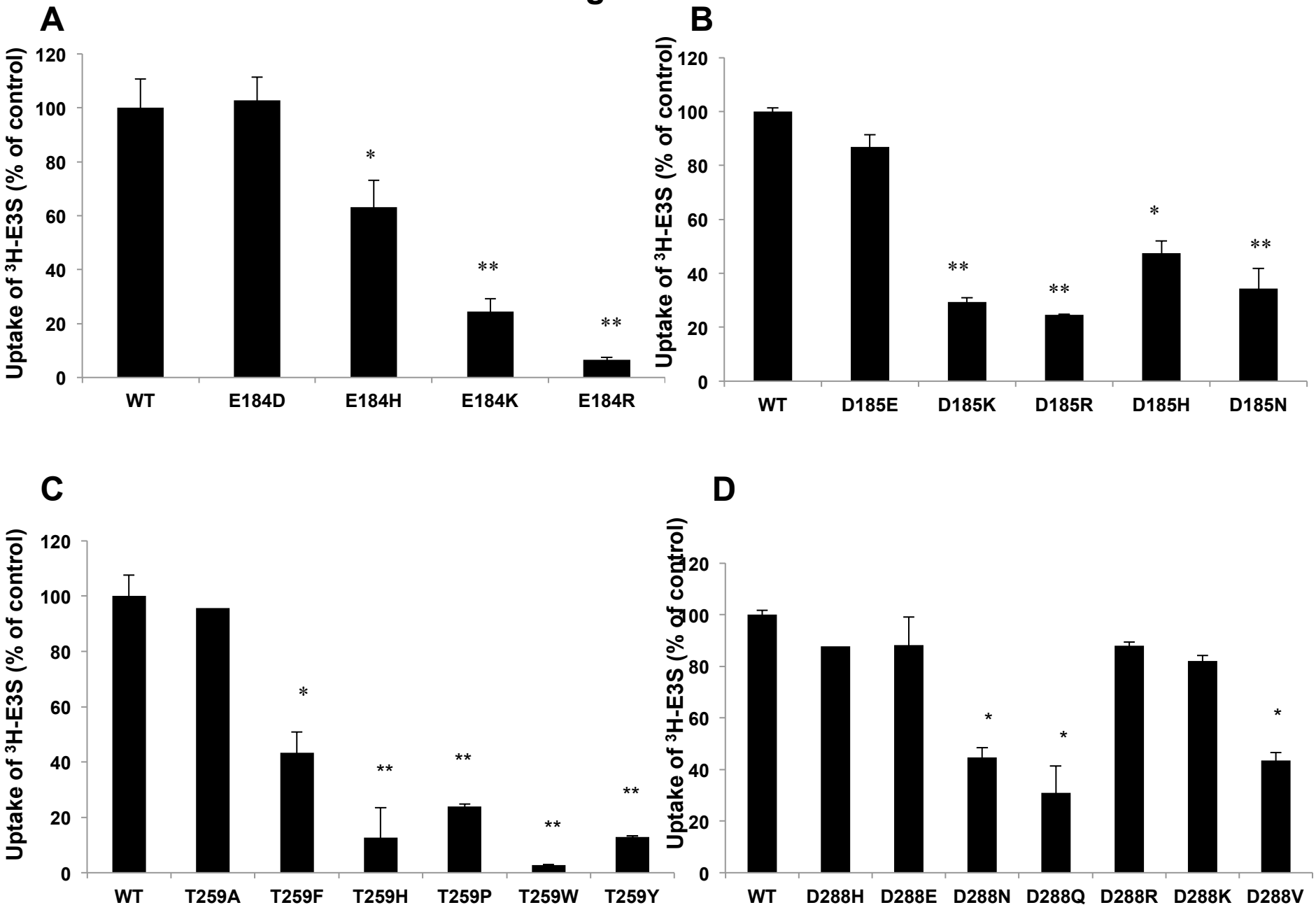
A
Uptake of ³H-E3S (% of control)
120
100
80
60
40
20
0
*
**
**
WT
E184D
E184H
E184K
E184R
B
Uptake of ³H-E3S (% of control)
120
100
80
60
40
20
0
**
**
*
**
WT
D185E
D185K
D185R
D185H
D185N
C
Uptake of ³H-E3S (% of control)
120
100
80
60
40
20
0
*
**
**
**
**
WT
T259A
T259F
T259H
T259P
T259W
T259Y
D
Uptake of ³H-E3S (% of control)
120
100
80
60
40
20
0
*
*
*
WT
D288H
D288E
D288N
D288Q
D288R
D288K
D288V

Figure 4

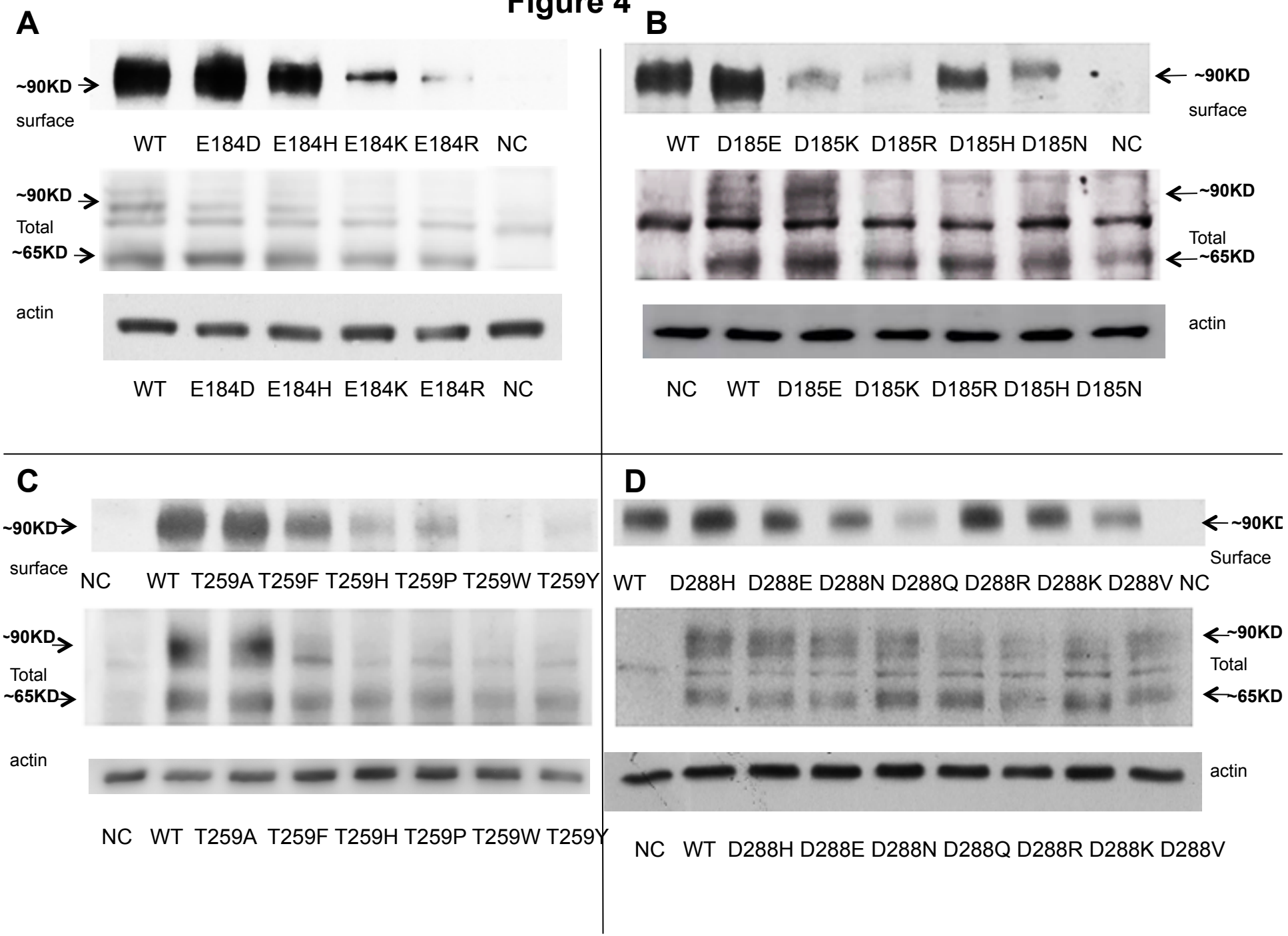
A
~90KD
surface
WT E184D E184H E184K E184R NC
~90KD
Total
~65KD
actin
WT E184D E184H E184K E184R NC
B
~90KD
surface
WT D185E D185K D185R D185H D185N NC
~90KD
Total
~65KD
actin
NC WT D185E D185K D185R D185H D185N
C
~90KD
surface
NC WT T259A T259F T259H T259P T259W T259Y
~90KD
Total
~65KD
actin
NC WT T259A T259F T259H T259P T259W T259Y
D
~90KD
Surface
WT D288H D288E D288N D288Q D288R D288K D288V NC
~90KD
Total
~65KD
actin
NC WT D288H D288E D288N D288Q D288R D288K D288V

Figure 5

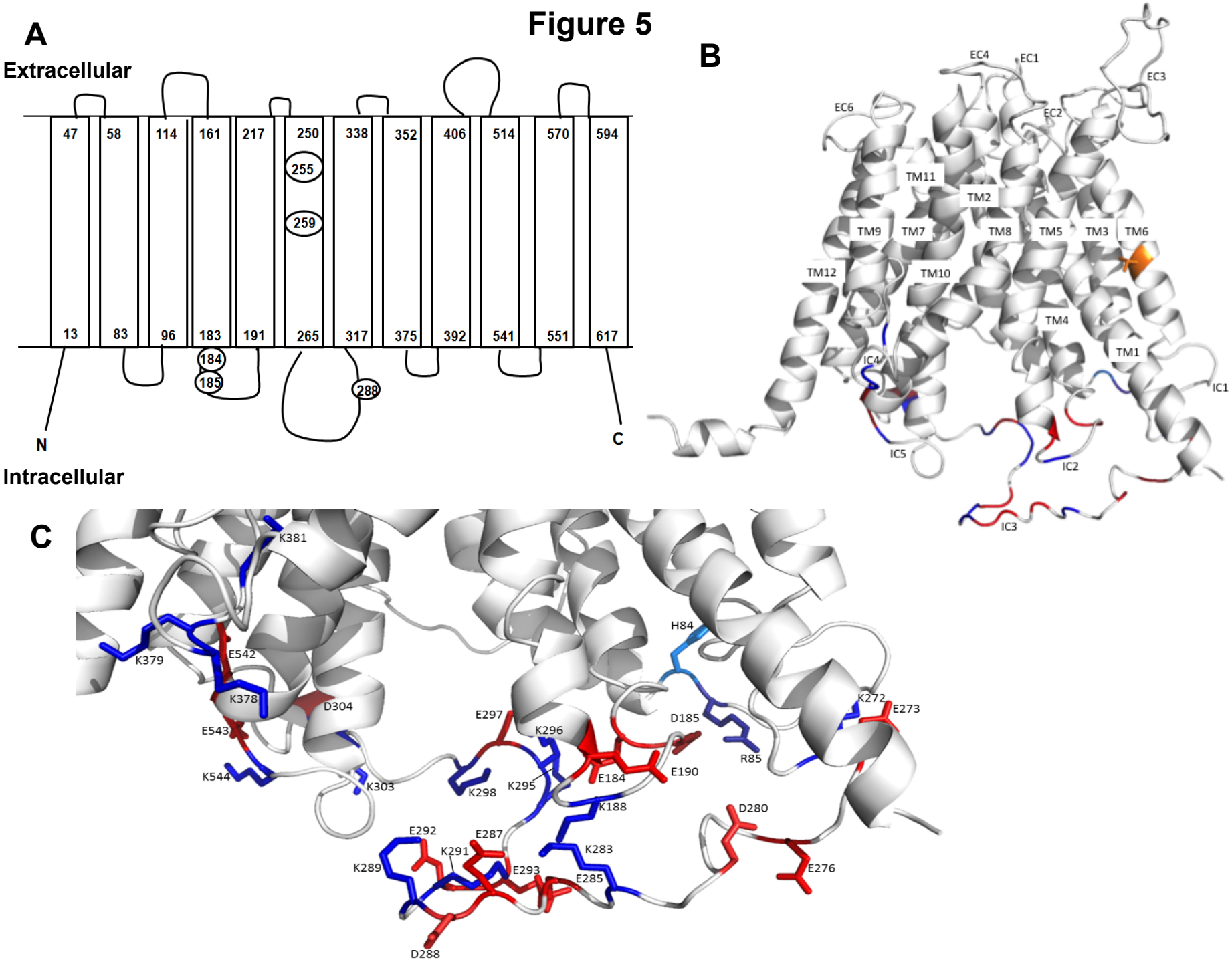
A
Extracellular
47
58
114
161
217
250
255
259
338
352
406
514
570
594
13
83
96
183
184
185
191
265
288
317
375
392
541
551
617
N
C
Intracellular
B
EC4
EC1
EC3
EC6
EC2
TM11
TM2
TM9
TM7
TM8
TM5
TM3
TM6
TM12
TM10
TM4
TM1
IC4
IC1
IC5
IC2
IC3
C
K381
K379
E542
K378
D304
E543
K544
K303
E297
K296
K298
K295
H84
D185
R85
E184
E190
K188
K272
E273
D280
E276
E292
E287
K291
K289
K283
E293
E285
D288